UDC519.63;519.684;539.87

Assylbekuly A.

International Kazakh – Turkish University named after H.A. Yassawe, Turkestan, Kazakhstan
e-mail:asylbekuly@mail.ru

Modeling of the complex impact on the hydrocarbon mixture

Abstract: The paper deals with modeling of mechanical activation and acoustic influence on the hydrocarbon mixture. The simulation of mechanical activation and acoustic impact on the hydrocarbon mixture is based on the three-dimensional Navier – Stokes equations conjunction with the continuity equation, and the equation for the concentration of the hydrocarbon mixture components in a rotary device. Mechanical activation and acoustic impact on the hydrocarbon mixture is organized by a special rotation of disks in a cylindrical area with the same speed, but in opposite directions. The obtained results contribute to the development of the new technologies of production, transportation and storage of oil and oil products, and may also be useful to industrial enterprises engaged in processing of hydrocarbon raw materials.
Key words: hydrocarbon mixture, complex effects, mechanical activation and acoustic impact, Navier-Stokes equations, rotary apparatus, rotating disk.

Introduction

Creating highly efficient and environmentally friendly technologies for the extraction, transportation and processing of oil is a very urgent task of the oil and gas sector of the Republic of Kazakhstan – the country with the raw material orientation of the economy. With the beginning of implementation of "State Program on Forced Industrial-Innovative Development of Kazakhstan for 2014 – 2019 years" and the plan "100 concrete steps to thirty of the world's leaders" [1, 2] is imperative to accumulate native research and development, the outcome of which may be applicable to develop new technologies for the production of light and heavy oil fractions. For such research one should include low energy impact on the hydrocarbons. Such influence allows without significant external energy costs (and sometimes it is produced by the use of internal reserves of the substance)restructure the starting material.These effects are investigated over the last 15 years, these include electromagnetic, electrical, magnetic, acoustic and vibration fields, and sometimes mechanical activation and thermo mechanical effects. Energy technology (acoustic, vibration, magnetic, etc.) are the most promising in view of their economy, effectiveness and accessibility. To such researches are devoted the works of famous scientists such as N.K Nadirov, A.A. Kalybaev, Y.A. Zaykin, R.F Zaykina etc . [3-10]. The above methods of influence on the oil is increasingly used in the oil industry, their use allows in a short period of time achieve a significant level of destruction the structure of oil's associates and maintains that level over time. Translation of raw materials in the active state allows you to more fully realize the potential of the raw materials and to achieve the increase of product yield or improve their quality indicators. In particular, the fractionation is a process for the separation of complex mixtures to more simples in the ideal case – to the individual components. Methods of separation are different and often based on the physical separation, or chemical surface properties of the oil components. Methods of separation are different and, most of all, based on the division of physical or chemical properties the oil components. Today, there are the following separation methods [11-12]: physical stabilization (degassing); distillation and rectification; distillation under vacuum; isotropic distillation; molecular distillation; adsorption; chromatography; the use of molecular sieve; extraction; Crystallization from solution; processing both chemicals and carbamide (in order to isolate normal paraffin).

One of the most promising areas of effective influence on the rheological properties of the oil and oil mixture is the complex impact on the treated hydrocarbon mixtures, where inresults, it is possible to obtain the required technological characteristics

in the production, transportation and processing of oil and oil mixture.

Application of the practical results of simulations of three-dimensional mathematical models of complex effects on the hydrocarbon mixture, and computational algorithms to the realization of the constructed mathematical models, the subsequent construction and design of the main technological equipment, may contribute to the development and creation of a more advanced and effective devices for joint mechanical activation and acoustic impact on hydrocarbon mixtures, depending on the assigned specific technological challenges.

Chemical reactions take place when the reactants are mixed at the molecular level at a sufficiently high temperature. Chemical reactions have occurred when the reactants are mixed at the molecular level at a sufficiently high temperature. It is known that at the level of micro-processes which are crucial for the molecular mixing, the energy dissipation of the turbulence to the heat becomes highly intermittent, i.e. concentrated in certain regions the small, relative to the total volume, areas whose dimensions are small in one or two directions (in three directions not simultaneously).

These regions occupy a delicate structure which can be vortex tubes, sheets and plates, the characteristic dimensions of which coincide with the order of the Kolmogorov microscale. Thin structures are responsible for the dissipation of turbulence to the heat. Therefore, we can assume that these reactants are mixed at a molecular level, thereby will create a space for the reaction of the unevenly distributed reagents .

Formulation of the problem

Here is a statement of objectives and implementation of simulation of mechanical activation and acoustic impact on hydrocarbon mixtures. The mathematical model of this process is based on the three-dimensional Navier-Stokes equation, the continuity equation, the equation for the concentration of the hydrocarbon mixture components in a cylindrical coordinate system. Figure 1 shows a cylindrical considered area within which the wheels are rotating against each other, R is radius of the cylinder, H is height. Rotating the dial clockwise and have the shape of the box is illustrated in green: ω_1 is angular velocity, $l_{f1} = 2\pi R_1 \varepsilon_2 / 360°$ is the length of the arc in the distance R_1, $L_{f1} = 2\pi R_2 \varepsilon_2 / 360°$ is length of the arc in the distance R_2. Turn counterclockwise drives also have the shape of the box and is illustrated in red: ω_2 is angular velocity, $l_{f2} = 2\pi R_3 \varepsilon_2 / 360°$ is the length of the arc in the distance R_3, $L_{f2} = 2\pi R_4 \varepsilon_2 / 360°$ is length of the arc in the distance R_4. Time for one period of rotation T_p.

(a) (b)

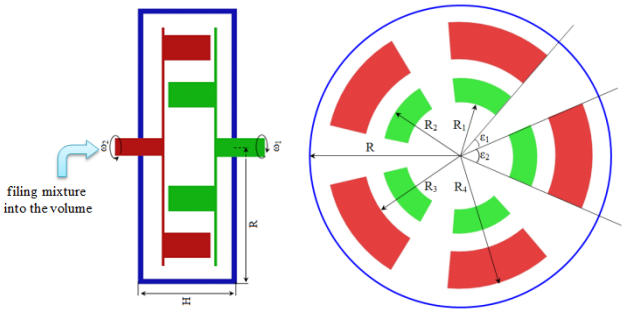

Figure 1– Illustration of the physical area

The process complex effects on the hydrocarbon mixture entering the cylinder, without chemical transformation which is required to simulate and implement. At the initial time the certain volume of fluid is pumped. The above-described rotation of the disc, as will be shown below, leads to the appearance within the area of the vortices, which in turn rotates around its horizontal and vertical axis of symmetry. The observed vortex formation leads to a change in the concentration distribution of the components inside the cylinder sweep.

Basic equations

For the mathematical description of mechanical activation and acoustic impact on the hydrocarbon mixture it is chosen averaged Navier – Stokes equation, the continuity equation and the concentration recorded in a cylindrical coordinate system (r, ε, z) [13-15]:

The equation of motion of the fluid for the r coordinate is:

$$\rho\left(\frac{\partial V_r}{\partial t}+V_r\frac{\partial V_r}{\partial r}+\frac{V_\varepsilon}{r}\frac{\partial V_r}{\partial \varepsilon}+V_z\frac{\partial V_r}{\partial z}-\frac{V_\varepsilon^2}{r}\right)=-\frac{\partial P}{\partial r}+$$
$$+\mu\left(\frac{1}{r}\frac{\partial}{\partial r}\left(r\frac{\partial V_r}{\partial r}\right)+\frac{1}{r^2}\frac{\partial^2 V_r}{\partial \varepsilon^2}+\frac{\partial^2 V_r}{\partial z^2}\right)-$$
$$-\rho\left(\frac{1}{r}\frac{\partial}{\partial r}\left(r\tau_{rr}\right)+\frac{1}{r}\frac{\partial}{\partial \varepsilon}\left(\tau_{r\varepsilon}\right)+\frac{\partial}{\partial z}\left(\tau_{rz}\right)-\frac{1}{r}\left(\tau_{rr}\right)\right)+$$
$$+\mu\left(-\frac{V_r}{r^2}-\frac{2}{r^2}\frac{\partial V_\varepsilon}{\partial \varepsilon}\right)+f_1+f_2 \tag{1}$$

The equation of motion of the fluid for the ε coordinate is:

$$\rho\left(\frac{\partial V_\varepsilon}{\partial t}+V_r\frac{\partial V_\varepsilon}{\partial r}+\frac{V_\varepsilon}{r}\frac{\partial V_\varepsilon}{\partial \varepsilon}+V_z\frac{\partial V_\varepsilon}{\partial z}+\frac{V_rV_\varepsilon}{r}\right)=-\frac{1}{r}\frac{\partial P}{\partial \varepsilon}+$$
$$+\mu\left(\frac{1}{r}\frac{\partial}{\partial r}\left(r\frac{\partial V_\varepsilon}{\partial r}\right)+\frac{1}{r^2}\frac{\partial^2 V_\varepsilon}{\partial \varepsilon^2}+\frac{\partial^2 V_\varepsilon}{\partial z^2}-\frac{V_\varepsilon}{r^2}+\frac{2}{r^2}\frac{\partial V_r}{\partial \varepsilon}\right)-$$
$$-\rho\left(\frac{\partial}{\partial r}\left(\tau_{\varepsilon r}\right)+\frac{1}{r}\frac{\partial}{\partial r}\left(\tau_{\varepsilon\varepsilon}\right)+\frac{\partial}{\partial z}\left(\tau_{\varepsilon z}\right)+\frac{2}{r}\tau_{r\varepsilon}\right)+f_1+f_2 \tag{2}$$

The equation of motion of the fluid for the z coordinate is:

$$\rho\left(\frac{\partial V_z}{\partial t}+V_r\frac{\partial V_z}{\partial r}+\frac{V_\varepsilon}{r}\frac{\partial V_z}{\partial \varepsilon}+V_z\frac{\partial V_z}{\partial z}\right)=-\frac{\partial P}{\partial z}+$$
$$+\mu\left(\frac{1}{r}\frac{\partial}{\partial r}\left(r\frac{\partial V_z}{\partial r}\right)+\frac{1}{r^2}\frac{\partial^2 V_z}{\partial \varepsilon^2}+\frac{\partial^2 V_z}{\partial z^2}\right)-$$
$$-\rho\left(\frac{1}{r}\frac{\partial}{\partial r}\left(r\tau_{zr}\right)+\frac{1}{r}\frac{\partial}{\partial \varepsilon}\left(\tau_{z\varepsilon}\right)+\frac{\partial}{\partial z}\left(\tau_{zz}\right)\right)+f_1+f_2 \tag{3}$$

The concentration equation:

$$\rho\left(\frac{\partial \overline{C}}{\partial t}+V_r\frac{\partial \overline{C}}{\partial r}+\frac{V_\varepsilon}{r}\frac{\partial \overline{C}}{\partial \varepsilon}+V_z\frac{\partial \overline{C}}{\partial z}\right)=k_C\left(\frac{1}{r}\frac{\partial}{\partial r}\left(r\frac{\partial \overline{C}}{\partial r}\right)+\frac{1}{r^2}\frac{\partial^2 \overline{C}}{\partial \varepsilon^2}+\frac{\partial^2 \overline{C}}{\partial z^2}\right)-$$
$$-\rho\left(\frac{1}{r}\frac{\partial}{\partial r}\left(rQ_r\right)+\frac{1}{r}\frac{\partial}{\partial \varepsilon}\left(Q_\varepsilon\right)+\frac{\partial}{\partial z}\left(Q_z\right)\right)+f_1+f_2; \tag{4}$$

The continuity equation:

$$\frac{\partial}{\partial r}\left(rV_r\right)+\frac{1}{r}\frac{\partial}{\partial \varepsilon}\left(rV_\varepsilon\right)+\frac{\partial}{\partial z}\left(rV_z\right)=0. \tag{5}$$

where, V_r, V_ε, V_z are velocity components, P is pressure, t is time, $\tau_{i,j}$ is rate of deformation tensor, *i, j* matches r, ε, z, C is concentration, f_1 is disc rotating clockwise, f_2 is disc rotating counterclockwise.

In Figure 2, disc f_1 is shown in green and the disc f_2 in red.

Initial (6) and boundary (7) conditions are following:

$$\begin{aligned} &V_r(t=0,\, r,\varepsilon,z)=0, \qquad V_\varepsilon(t=0,\, r,\varepsilon,z)=0,\\ &V_z(t=0,\, r,\varepsilon,z)=0, \qquad C(t=0,\, r,\varepsilon,z)=0. \end{aligned} \tag{6}$$

$$\left.\begin{aligned} &V_r(t,r=0,\varepsilon,z)=V_r(t,\Delta r,\varepsilon,z), \quad V_r(t,r,\varepsilon=0,z)=V_r(t,r,\varepsilon=2\pi,z),\\ &V_\varepsilon(t,r=0,\varepsilon,z)=V_\varepsilon(t,\Delta r,\varepsilon,z), \quad V_\varepsilon(t,r,\varepsilon=0,z)=V_\varepsilon(t,r,\varepsilon=2\pi,z),\\ &V_z(t,r=0,\varepsilon,z)=V_z(t,\Delta r,\varepsilon,z), \quad V_z(t,r,\varepsilon=0,z)=V_z(t,r,\varepsilon=2\pi,z),\\ &V_r(t,r=R,\varepsilon,z)=0, \quad V_r(t,r,\varepsilon,z=0)=0, \quad V_r(t,r,\varepsilon,z=H)=0,\\ &V_\varepsilon(t,r=R,\varepsilon,z)=0, \quad V_\varepsilon(t,r,\varepsilon,z=0)=0, \quad V_\varepsilon(t,r,\varepsilon,z=H)=0,\\ &V_z(t,r=R,\varepsilon,z)=0, \quad V_z(t,r,\varepsilon,z=0)=0, \quad V_z(t,r,\varepsilon,z=H)=0,\\ &C(t,r=0,\varepsilon,z)=1, \quad C(t,r,\varepsilon=0,z)=C(t,r,\varepsilon=2\pi,z),\\ &C(t,r=R,\varepsilon,z)=0, \quad C(t,r,\varepsilon,z=0)=0, \quad C(t,r,\varepsilon,z=H)=0. \end{aligned}\right\} \tag{7}$$

In order to eliminate the uncertainties, appearing in (1) – (5) at $r=0$, the carried out conversion allows to display the physical area (r, ε, z) on computing (x_1, x_2, x_3), having the shape of a cube [14], by using the formula: $r=e^{x_1}$, $\varepsilon=\Psi x_2$, $z=H x_3$.

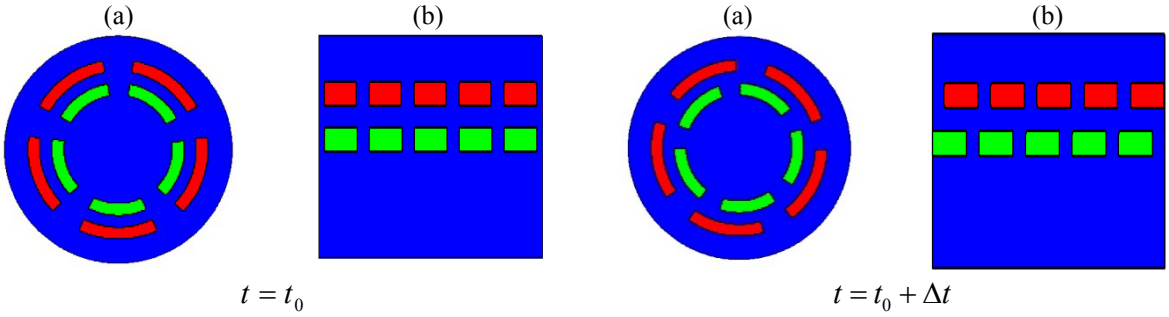

Figure 2 – Locations of rotating disks in the physical region (a), in the computing area (b) at different times

After carrying out this transformation it is necessary to make major dimensionless equation. For this purpose, selected the characteristic values of the tangential velocity, ωL_1 dimensions discrete area: L_1 is the length of the field along the axis of x_1, L_2 is the length of the field along the axis of x_2, L_3 is the length of the field along the axis of x_3.

Using these parameters, we introduce the following notation:

$$x_1^* = \frac{x_1}{L_1}, \quad x_2^* = \frac{x_2}{L_2}, \quad x_3^* = \frac{x_3}{L_3},$$

$$\overline{u}_1^* = \frac{u_1}{\omega L_1}, \quad \overline{u}_2^* = \frac{u_2}{\omega L_1}, \quad \overline{u}_3^* = \frac{u_3}{\omega L_1},$$

$$\tau = \frac{t\omega}{L_2}, \quad \overline{p}^* = \frac{p}{\rho\omega^2 L_1^{\,2}}, \quad \frac{1}{\mathrm{Re}} = \frac{\nu}{L_1^{\,2}\omega}, \tag{8}$$

$$\sigma(x_1) = \frac{1}{e^{x_1}},$$

where Re is Reynolds number. Sign of the "star" means a dimensionless quantity. Given the equalities $L_1 = 1,\ L_2 = 1,\ L_3 = 1$ which determine the size of the computational domain $[0;1]\times[0;1]\times[0;1]$, the initial equations are converted to the simpler form given below.

Expressing all the values in (1) – (5) through the relevant dimensionless quantities of (8) and dropping the mark "star" for dimensionless quantities a system of equations can be reduced to the following form:

$$\frac{\partial\overline{u}_1}{\partial\tau} + \sigma L_2\overline{u}_1\frac{\partial\overline{u}_1}{\partial x_1} + \sigma\frac{L_1}{\Psi}\overline{u}_2\frac{\partial\overline{u}_1}{\partial x_2} + \frac{(L_2L_1)}{L_3}\frac{\overline{u}_3}{H}\frac{\partial\overline{u}_1}{\partial x_3} - \sigma L_2L_1(\overline{u}_2)^2 = -\sigma\frac{\partial\overline{p}}{\partial x_1} +$$

$$+L^*\frac{1}{\mathrm{Re}}\left[\begin{array}{l}\sigma^2\dfrac{\partial}{\partial x_1}\left(\dfrac{\partial\overline{u}_1}{\partial x_1}\right)+\sigma^2\dfrac{1}{\Psi^2}\dfrac{L_1^{\,2}}{L_2^{\,2}}\dfrac{\partial}{\partial x_2}\left(\dfrac{\partial\overline{u}_1}{\partial x_2}\right)+\\ +\dfrac{1}{H^2}\dfrac{L_1^{\,2}}{L_3^{\,2}}\dfrac{\partial}{\partial x_3}\left(\dfrac{\partial\overline{u}_1}{\partial x_3}\right)-\\ -\sigma^2L_1^{\,2}\overline{u}_1-\sigma^2\dfrac{2}{\Psi}\dfrac{L_1^{\,2}}{L_2^{\,2}}\dfrac{\partial\overline{u}_2}{\partial x_2}\end{array}\right]+ \tag{9}$$

$$+\sigma^2\frac{\partial}{\partial x_1}\left(-\frac{1}{\sigma}\tau_{11}\right)+\sigma\frac{L_1}{\Psi}\frac{\partial}{\partial x_2}(-\tau_{12})+\frac{L_1}{H}\frac{\partial}{\partial x_3}(-\tau_{13})-\sigma(-\tau_{22})+f_1+f_2,$$

$$\frac{\partial \overline{u}_2}{\partial \tau}+\sigma L_2\overline{u}_1\ \frac{\partial \overline{u}_2}{\partial x_1}+\sigma\frac{L_1}{\Psi}\overline{u}_2\ \frac{\partial \overline{u}_2}{\partial x_2}+\frac{\left(L_2L_1\right)}{L_3}\frac{\overline{u}_3}{H}\frac{\partial \overline{u}_2}{\partial x_3}+\sigma L_2L_1\left(\overline{u}_1\ \overline{u}_2\right)=-\sigma\frac{1}{\Psi}\frac{\partial \overline{p}}{\partial x_2}+$$

$$+L_2\frac{1}{\mathrm{Re}}\left[\begin{array}{l}\sigma^2\frac{\partial}{\partial x_1}\left(\frac{\partial \overline{u}_2}{\partial x_1}\right)+\sigma^2\frac{1}{\Psi^2}\frac{L_1^{\ 2}}{L_2^{\ 2}}\frac{\partial}{\partial x_2}\left(\frac{\partial \overline{u}_2}{\partial x_2}\right)+\\ +\frac{1}{H^2}\frac{L_1^{\ 2}}{L_3^{\ 2}}\frac{\partial}{\partial x_3}\left(\frac{\partial \overline{u}_2}{\partial x_3}\right)-\sigma^2L_1^{\ 2}\overline{u}_2+\sigma^2\frac{2}{\Psi}\frac{L_1^{\ 2}}{L_2}\frac{\partial \overline{u}_1}{\partial x_2}\end{array}\right]+ \tag{10}$$

$$+\frac{\partial}{\partial x_1}\left(-\tau_{21}\right)+\sigma\frac{L_1}{\Psi}\frac{\partial}{\partial x_2}\left(-\tau_{22}\right)+\frac{L_1}{H}\frac{\partial}{\partial x_3}\left(-\tau_{23}\right)+2\sigma\left(-\tau_{12}\right)+f_1+f_2,$$

$$\frac{\partial \overline{u}_3}{\partial \tau}+\sigma L_2\overline{u}_1\ \frac{\partial \overline{u}_3}{\partial x_1}+\sigma\frac{L_1}{\Psi}\overline{u}_2\ \frac{\partial \overline{u}_3}{\partial x_2}+\frac{\left(L_2L_1\right)}{L_3}\frac{\overline{u}_3}{H}\frac{\partial \overline{u}_3}{\partial x_3}=-\frac{1}{H}\frac{\partial \overline{p}}{\partial x_3}+$$

$$+L_2\frac{1}{\mathrm{Re}}\left[\sigma^2\frac{\partial}{\partial x_1}\left(\frac{\partial \overline{u}_3}{\partial x_1}\right)+\sigma^2\frac{1}{\Psi^2}\frac{L_1^{\ 2}}{L_2^{\ 2}}\frac{\partial}{\partial x_2}\left(\frac{\partial \overline{u}_3}{\partial x_2}\right)+\frac{1}{H^2}\frac{L_1^{\ 2}}{L_3^{\ 2}}\frac{\partial}{\partial x_3}\left(\frac{\partial \overline{u}_3}{\partial x_3}\right)\right]+ \tag{11}$$

$$+\sigma^2\frac{\partial}{\partial x_1}\left(-\frac{1}{\sigma}\tau_{31}\right)+\sigma\frac{L_1}{L}\frac{\partial}{\partial x_2}\left(-\tau_{32}\right)+\frac{L_1}{H}\frac{\partial}{\partial x_3}\left(-\tau_{33}\right)+f_1+f_2.$$

The equation for concentration:

$$\frac{\partial \overline{C}}{\partial \tau}+\overline{u}_1\ L_2\sigma\frac{\partial \overline{C}}{\partial x_1}+\overline{u}_2\sigma\frac{L_1}{\Psi}\frac{\partial \overline{C}}{\partial x_2}+\overline{u}_3\ \frac{1}{\Gamma}\frac{\partial \overline{C}}{\partial x_3}=$$

$$+\frac{1}{Pe}\left[\sigma^2\frac{\partial}{\partial x_1}\left(\frac{\partial \overline{C}}{\partial x_1}\right)+\sigma^2\frac{1}{\Psi^2}\frac{L_1^{\ 2}}{L_2^{\ 2}}\frac{\partial}{\partial x_2}\left(\frac{\partial \overline{C}}{\partial x_2}\right)+\frac{1}{\Gamma^2}\frac{\partial}{\partial x_3}\left(\frac{\partial \overline{C}}{\partial x_3}\right)\right]+ \tag{12}$$

$$+\sigma^2\frac{\partial}{\partial x_1}\left(\sigma Q_1\right)+\frac{1}{\Psi}\sigma\frac{\partial}{\partial x_2}\left(Q_2\right)+\frac{1}{\Gamma}\frac{\partial}{\partial x_3}\left(Q_3\right)+f_1+f_2+R_\alpha.$$

As a result, the continuity equation takes the following form:

$$\sigma^2 \frac{\partial}{L_1 \partial x_1}\left(\frac{1}{\sigma}\bar{u}_1\right)+\frac{1}{\Psi}\sigma\frac{\partial}{L_2\partial x_2}\left(\bar{u}_2\right)+\frac{1}{H}\frac{\partial}{L_3\partial x_3}\left(\bar{u}_3\right)=0. \tag{13}$$

where,

$$\tau_{ij}=\overline{u_i u_j}-\bar{u}_i\bar{u}_j,$$

$$Q_j=\overline{u_j C}-\bar{u}_j\bar{C}.$$

In (9) – (11) subgrid Reynolds stress is presented, which is used to simulate the following viscous model:

$$\tau_{ij}-\frac{\delta_{ij}}{3}\tau_{kk}=-2\nu_T\bar{S}_{ij}, \tag{14}$$

where the turbulent viscosity is represented as

$$\nu_T=\left(C_S\Delta\right)^2\left(2\bar{S}_{ij}\bar{S}_{ij}\right)^{1/2} \tag{15}$$

$$\bar{S}_{ij}=\frac{1}{2}\left(\frac{\partial\bar{u}_i}{\partial x_j}+\frac{\partial\bar{u}_j}{\partial x_i}\right) \tag{16}$$

$\delta_{ij}=\begin{cases}1, i=j\\0, i\neq j\end{cases}$ is the Kronecker symbol, C_S is the coefficient for this problem which is assumed to be – 0.10 [15], $\Delta=\left(e^{x_1}\,\Delta x_1\,\Delta x_2\,\Delta x_3\right)^{1/3}$ – the characteristic length of the filter, which has an order of the grid spacing, $\Delta x_1=1/N_1$, $\Delta x_2=1/N_2$, $\Delta x_3=1/N_3$ are step in the direction of the grid calculated respective to axes $\left(x_1,x_2,x_3\right)$, N_1, N_2, N_3 is the number of nodes.

Thus, the problem (1) – (5) is replaced by the equations (9) – (13), i.e. the solution will be carried out in the Cartesian coordinate system, and the initial and boundary conditions for this statement correspond to the conditions (6) – (7). Note also that the condition of periodicity for the speed of the propeller:

$$V_p\left(\tau+\Delta\tau k, x_1, x_2+\Delta x_2, x_3\right)=$$
$$=V_p\left(\tau, x_1, x_2, x_3\right),\ 0\le k\le T_p,$$

which indicates a change in the location of the propeller blades when they are displayed on the Cartesian plane. This $\Delta\tau=1/T_p$.

$$Q_j=\overline{u_j C}-\bar{u}_j\bar{C} \tag{17}$$

Other spatially compact filters, including asymmetric filters, with comparable yield with change results in expansion coefficients as indicated below. It is assumed that the filtering operation is performed for the spatial derivatives, which is true for spatially homogeneous filter [16].

The traditional procedure is to use a large-scale and the physical parameters for the simulation unclosed terms in the equation (17). The shape of the diffusion gradient:

$$Q_j=-k_{TC}\frac{\partial C}{\partial x_j} \tag{18}$$

where k_{TC} is a scalar vortex diffusivity. In the large eddy simulation model, common practice is to use Smagorinsky model, which is expressed as follows:

$$k_{TC} = \frac{1}{\sigma_T}(C_s\Delta)^2\left(\overline{S}_{ij}\overline{S}_{ij}\right)^{1/2}\overline{S}_{ij} \qquad (19)$$

where C_s is constant Smagorinsky coefficient, σ_T is turbulent Schmidt number (usually chosen equal to 1) and S_{ij} is found tensor speed voltage.

Numerical method

For solving the problem in view of above mentioned suggested models of turbulent motion of an incompressible fluid in a cylindrical domain, the splitting scheme by physical parameters is used. Its implementation in stages I – IV is shown below:

$$\text{I.}\ \frac{\vec{u}^{\,*}-\vec{u}^{\,n}}{\tau} = -\left(\vec{u}^{\,n}\nabla\vec{u}^{\,*} - \nu\Delta\vec{u}^{\,*}\right),$$

$$\text{II.}\ \Delta p = \frac{\nabla\vec{u}^{\,*}}{\tau},$$

$$\text{III.}\ \frac{\vec{u}^{\,n+1}-\vec{u}^{\,*}}{\tau} = -\nabla p.$$

$$\text{IV.}\ \frac{\vec{C}^{n+1}-\vec{C}^{n}}{\tau} = -\left(\vec{u}^{\,n+1}\nabla\vec{C}^{n+1} - \frac{1}{\mathrm{Pe}}\Delta\vec{C}^{n+1}\right),$$

At the first stage the transfer of momentum is carried out only by convection and diffusion. The intermediate velocity field is calculated by the method of fractional steps, using the sweep method. At the second stage, pressure is calculated by using already founded intermediate velocity field. At the third step we assume that the transfer is only carried out by the pressure gradient. At the fourth step the concentration is calculated by using finite velocity fields.

The intermediate velocity field is calculated by using the method of fractional steps. Sweep method for finding values of the intermediate velocity field used at the each step of the method of fractional steps.

Numerical results

The numerical model allows to describe the turbulent motion of the hydrocarbon mixture in a rotary machine with rotating discs. Calculations are made for different speeds of drives attached to the rotor and rotating in the opposite direction. For calculation the size of the mesh 128 * 256 * 64 is used. The $\Delta\tau$ time step's values are equal to 0.0005 and 0.001, i.e. the first value is two times less than the second one. Main physical value of $\Delta\tau$ time is is a single rotation of the disk, i.e., the smaller the time, the faster the speed of rotation of rotor. With an increase of this magnitude the rotor speed is reduced.

Also, for the study of fluid dynamics we produced the calculations for different values of the Reynolds number: Re = 2500, Re = 5000. It was determined that the increase of Re number results in the appearance vortices.

As a result of the numerical realization of the problem, the following results, an illustration of which is shown in Figures 3 – 10, demonstrates the distribution of the kinetic energy and dynamics change of concentration of the hydrocarbon mixture components for different values of the Reynolds number Re = 2500, Re = 5000 and for different values of the time step, $\Delta\tau = 0.0005$, $\Delta\tau = 0.001$.

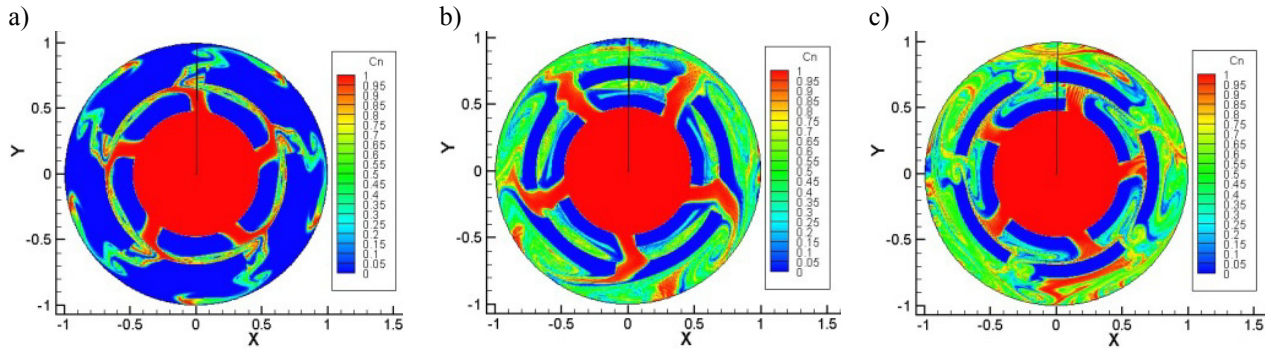

Figure 3 – Dynamic change of hydrocarbon components concentration under condition of $\mathrm{Re} = 2500,\ \Delta\tau = 0.001$ at time point: $a)\ t = 0.25,\ b)\ t = 1.0,\ c)\ t = 1.5$

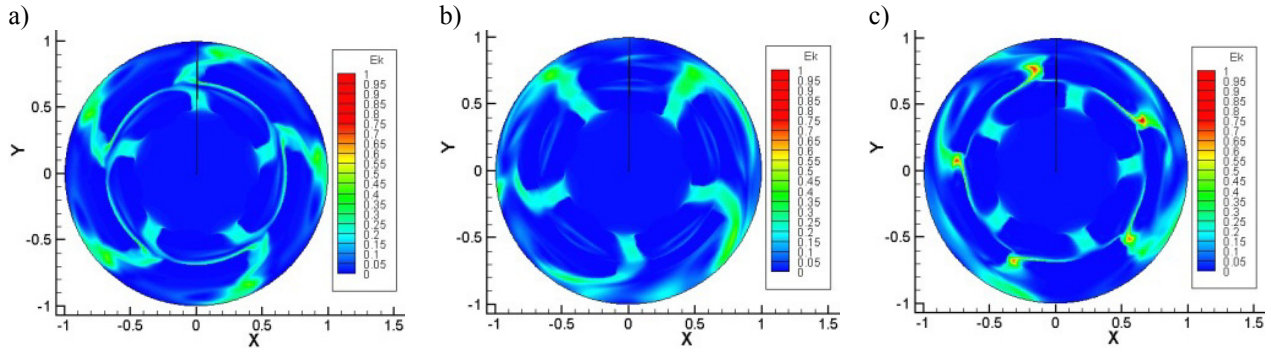

Figure 4 – The distribution of the kinetic energy under condition of $\mathrm{Re} = 2500,\ \Delta\tau = 0.001$ at time point: $a)\ t = 0.25,\ b)\ t = 1.0,\ c)\ t = 1.5$

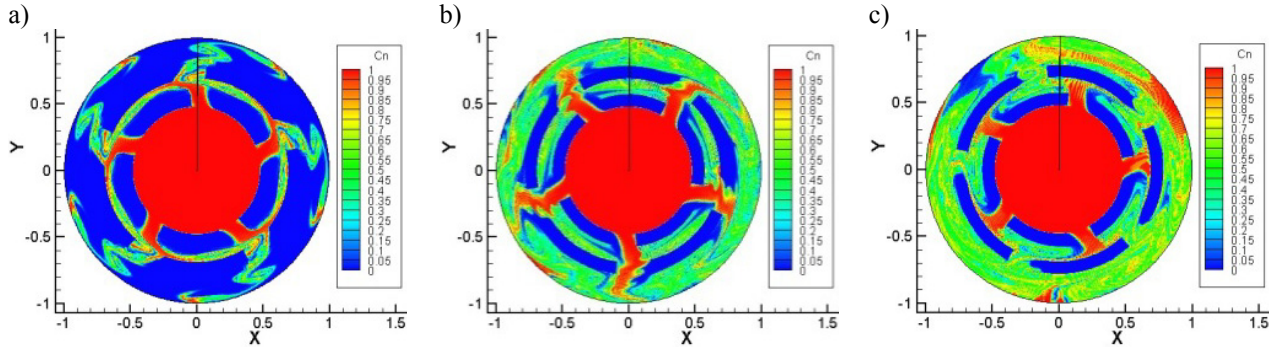

Figure 5 – Dynamic change of hydrocarbon components concentration under condition of $\mathrm{Re} = 5000,\ \Delta\tau = 0.001$ at time point: $a)\ t = 0.25,\ b)\ t = 1.0,\ c)\ t = 1.5.$

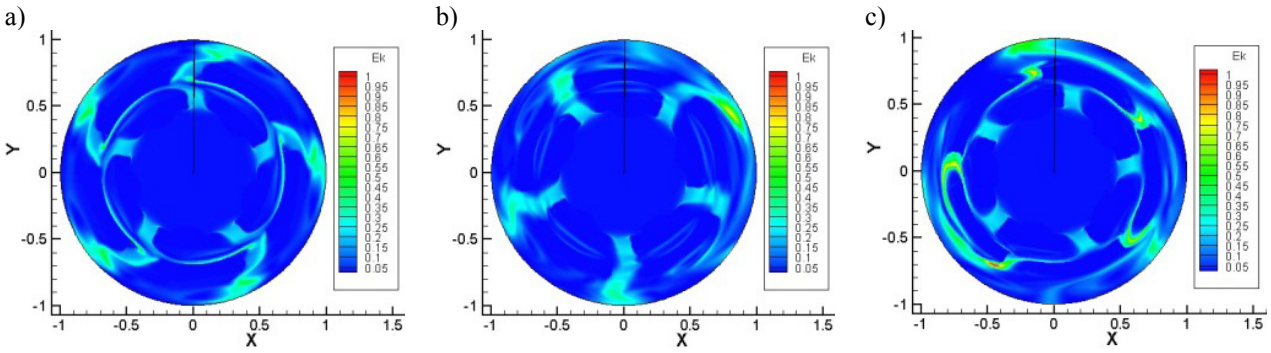

Figure 6 – The distribution of the kinetic energy under condition of $\mathrm{Re} = 5000,\ \Delta\tau = 0.001$ at time point: $a)\ t = 0.25,\ b)\ t = 1.0,\ c)\ t = 1.5.$

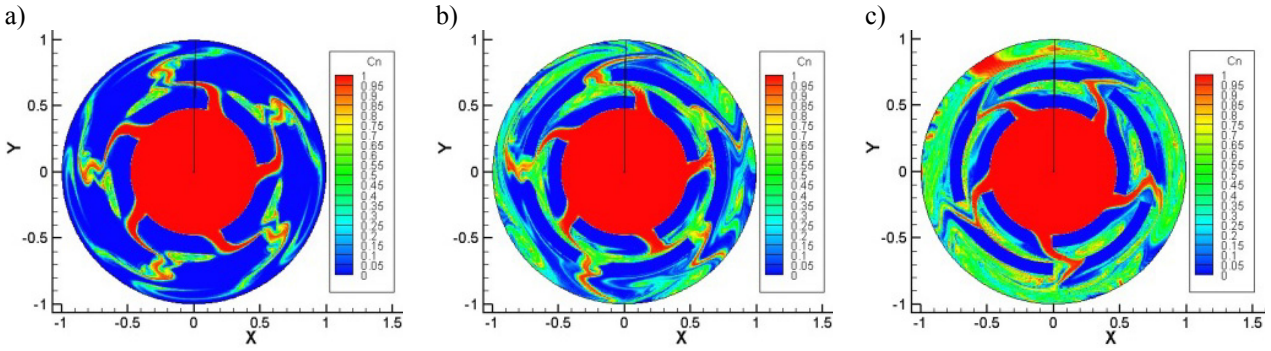

Figure 7 – Dynamic change of hydrocarbon components concentration under condition of $\mathrm{Re} = 2500,\ \Delta\tau = 0.0005$ at time point: $a)\ t = 0.25,\ b)\ t = 1.0,\ c)\ t = 1.5.$

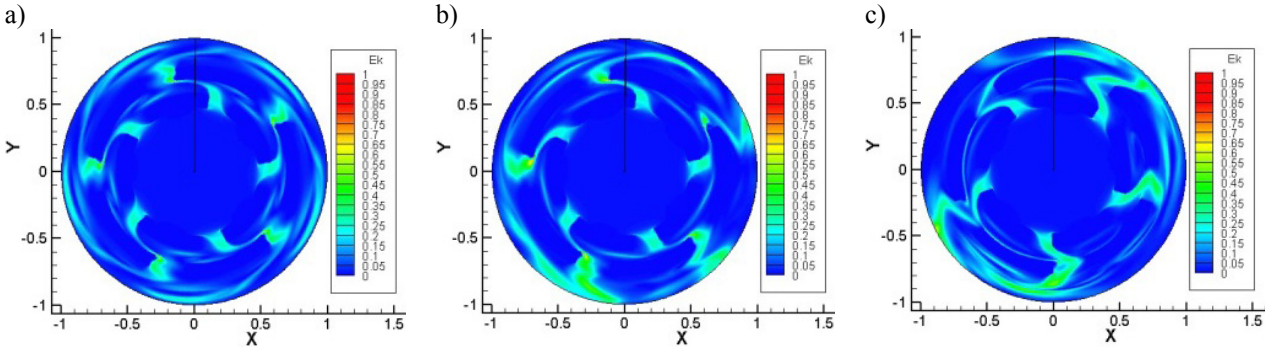

Figure 8 – The distribution of the kinetic energy under condition of $\mathrm{Re} = 2500,\ \Delta\tau = 0.0005$ at time point: $a)\ t = 0.25,\ b)\ t = 1.0,\ c)\ t = 1.5.$

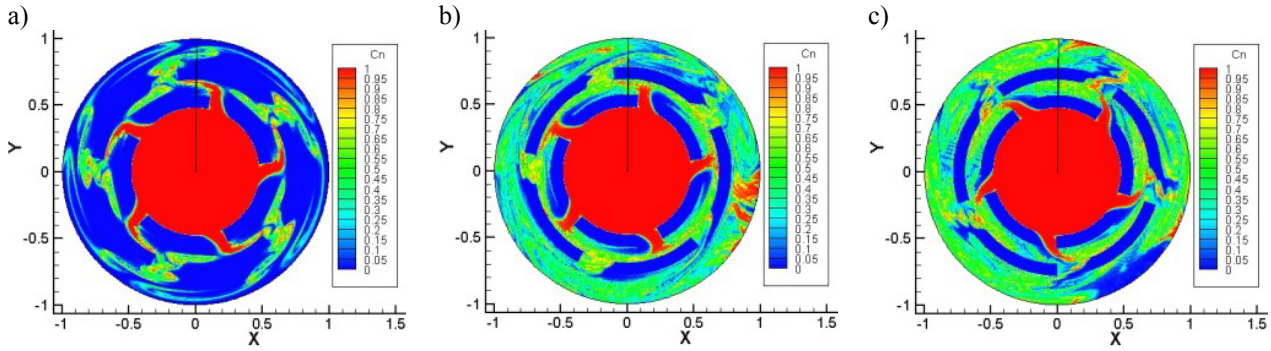

Figure 9 – Dynamic change of hydrocarbon components concentration under condition of $\mathrm{Re} = 5000,\ \Delta\tau = 0.0005$ at time point: $a)\ t = 0.25,\ b)\ t = 1.0,\ c)\ t = 1.5.$

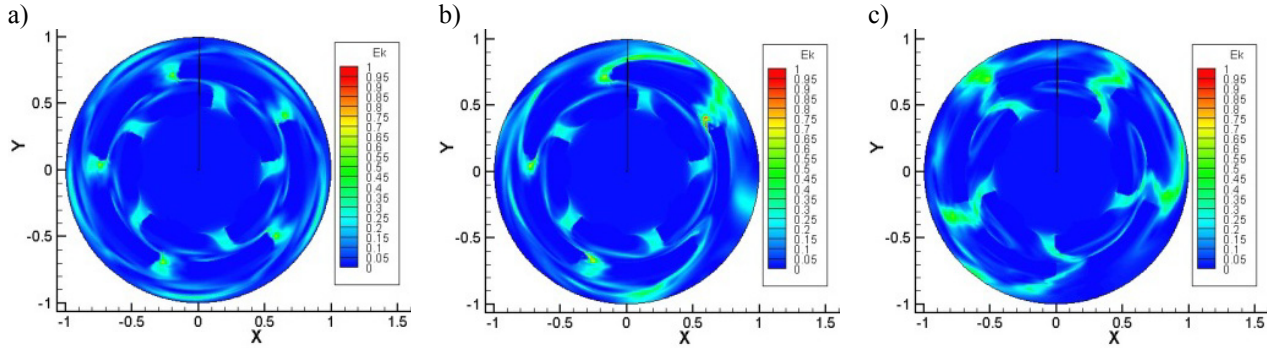

Figure 10 – The distribution of the kinetic energy under condition of $\mathrm{Re} = 5000,\ \Delta\tau = 0.0005$ at time point: $a)\ t = 0.25,\ b)\ t = 1.0,\ c)\ t = 1.5.$

The solution of modeling the mechanical activation and acoustic impact on the hydrocarbon mixture showed that at a certain speed drives vortex formation is observed, leading to the change in the concentration distribution inside the observed area. With increasing speed of disks the number of small vortices increases.

Implementation of the developed mathematical models for complex effects on the hydrocarbon mixture gives an opportunity to examine the impact of the process, provided a variety of tasks of disc rotation speed, as well as search for optimal speed, in order to be able to catch the eddy formation. It should be noted, that the slow, along with the rapid rotation of disks does not result to the above-described influence on a hydrocarbon mixture.

Thus, by solving the Navier – Stokes equation, the continuity equation, equation of concentration in a rotary machine with rotating discs the numerical simulation of the dynamics of complex influence on the hydrocarbon mixture are carried out.

References

1. Gosudarstvennaja programma industrial'no-innovacionnogo razvitija Respubliki Kazahstan na 2015-2019 gody // Sobranie zakonodatel'stva RK. – 2015. – Vol.89.

2. Plan Nazarbaeva:100 konkretnyh shagov k tridcatke mirovyh liderov // N.A. Nazarbaev // Novosti Kazahstana [Jelektronnyj resurs]. Rezhim dostupa: http://www.zakon.kz

3. Zaykin Ju.A., Zaykina R.F., Nadirov N.K. Glubokaja konversija uglevodorodnogo syr'ja radiacionno-iniciirovannym krekingom // Neft' i gaz. – 2004. – Vol. 4. – P. 152-159.

4. Kalybaev A.A. Teorija i praktika holodnogo krekinga // Vestnik IARK. – 2003. – № 2 (10). – P. 132-137.

5. Loskutova Ju.V. Vlijanie magnitnogo polja na reologicheskie svojstva neftej // Tomsk, 2003. – 138 p.

6. Nadirov N.K., Vysokovjazkie nefti i prirodnye bitumy. – Almaty, 2001.– Vol.5. – 269 p.

7. Buchachenko A.L. Magnitnye jeffekty v himicheskih reakcijah // Uspehi himii. – 1977. – Vol.45. – P.761-793.

8. Lesin V.I. Mehanizm vozdejstvija magnitnyh polej // Neftjanoe hozjajstvo. – 1994. – Vol. 6. – P. 24-27.

9. Borsuckij Z.R. Issledovanija mehanizma magnitnoj obrabotki neftej na osnove rezul'tatov laboratornyh i promyslovyh ispytanij // Z.R. Borsuckij, S.E. Il'jasov // Neftepromyslovoe delo. – 2002. – Vol.8. – P.28-37.

10. Yakovlev V.A., Zavarukhin S.G., V.T. Kuzavov, Stebnovskii S.V., Malykh N.V., Mal'tsev L.I., Parmon V.N. A study of chemical transformations of organic compounds under the action of cavitation // Effect of external factors on physicochemical transformations.–2010. – Vol.4. – P. 227-234.

11. Adamowski J.C., Buiochi F., Simon C., Silva E.C.N. and Sigelmann R. Ultrasonic Measurement of Density of Liquids // The Journal of the Acoustical Society of America. – 1995. – Vol. 97– P. 354-361.

12. Kam'janov V.F. Issledovanija v oblasti himii vysokomolekuljarnyh soedinenij nefti // Sb. Problemy i dostizhenija v issledovanii nefti.– Tomsk: TNC SO AN SSSR, 1990. – P. 65-99.

13. Abdibekov U.S., Zhakebaev D.B., Zhumagulov B.T. Modelirovanie turbulentnogo peremeshivanija odnorodnoj zhidkosti metodom krupnyh vihrej // Vychislitel'nye tehnologii. – 2009 – Vol.14, No 2. – P.3-12.

14. Belocerkovskij, O.M. Prjamoe chislennoe modelirovanie «perehodnyh» techenij gaza i zadach turbulentnosti // Mehanika turbulentnyh potokov. Moskva, – 1980. –P. 70 – 109.

15. Hartmann H., Derksen J.J., Van den Akker, H.E.A. Macro – instability uncovered in a Rushton turbine stirred tank // A.I.Ch.E. Journal. – 2004. – № 50(10). – P. 2383–2393.

16. S. Ghosal and P. Moin. The basic equations foe the large-eddy simulation of turbulent flows in complex geometry// J. Comp. Phys. – 1995. – Vol. 84. – 118 p.